

*Ab initio* theory of polar semiconductor surfaces.II.  $(2 \times 2)$  reconstructions and related phase transitions of GaAs( $\bar{1}\bar{1}\bar{1}$ )

E. Kaxiras, Y. Bar-Yam, and J. D. Joannopoulos

*Department of Physics, Massachusetts Institute of Technology, Cambridge, Massachusetts 02139*

K. C. Pandey

*IBM Thomas J. Watson Research Center, P.O. Box 218, Yorktown Heights, New York 10598*

(Received 20 January 1987)

The  $(2 \times 2)$  reconstructions of GaAs( $\bar{1}\bar{1}\bar{1}$ ) are studied with use of a theoretical approach based on the calculation of the total energy in the context of density-functional theory and the pseudopotential approximation. New models are proposed for the As-rich and Ga-rich reconstructions. The relative chemical potential plays a crucial role in determining the lowest-energy configuration. The total-energy versus chemical-potential curves indicate the possibility of phase transitions between different configurations. One such transition concerning the experimentally observed  $(\sqrt{19} \times \sqrt{19})$  reconstruction can be explained as an intermediate phase between the proposed low-energy  $(2 \times 2)$  reconstructions.

## I. INTRODUCTION

Polar semiconductor surfaces exhibit a variety of complicated reconstruction patterns as well as structural phase transitions between the different reconstructions. These surface phenomena are poorly understood despite the large amount of experimental information that has been gathered about representative polar surfaces of III-V compound semiconductors.<sup>1-10</sup> In particular, the ( $\bar{1}\bar{1}\bar{1}$ ) surface of GaAs has several stable reconstructions: Two different  $(2 \times 2)$  patterns have been observed<sup>1,2,9</sup> as well as a  $(\sqrt{19} \times \sqrt{19})$ ,<sup>1,3,4</sup> a  $(3 \times 3)$ ,<sup>9</sup> and a  $(\sqrt{3} \times \sqrt{3})$ .<sup>4</sup> A transition between the  $(2 \times 2)$  and  $(\sqrt{19} \times \sqrt{19})$  phases is readily obtained by varying the temperature or the relative As- to Ga-arrival rate during the molecular-beam-epitaxy (MBE) growth of this surface.<sup>1</sup> At present various models exist that attempt to describe the mentioned surface reconstructions<sup>10-12</sup> but none has been unequivocally confirmed as the proper atomic geometry. Furthermore, there is no satisfactory understanding of the mechanism that induces the observed structural transitions between the different phases.

In a previous paper (paper I),<sup>13</sup> a first-principles, self-consistent theoretical method for dealing with polar compound semiconductor surfaces was described in detail; paper I also contained an application of the methodology to the  $(2 \times 2)$  surface reconstructions of GaAs(111). In the present work the same method will be applied to the  $(2 \times 2)$  reconstructions of GaAs( $\bar{1}\bar{1}\bar{1}$ ). By using this methodology we will attempt to find the appropriate lowest-energy surface reconstruction and gain some insight into the phase-transition mechanisms by considering the combination of low-energy structural units.

The format of this paper is as follows: Section II contains a very brief review of the methodology. Section III discusses the geometric features of the different reconstruction models for the ( $\bar{1}\bar{1}\bar{1}$ ) surface, and the total energy of each model. Section IV discusses the effect of the

relative chemical potential of Ga and As atoms on the total energies. Finally, Sec. V makes contact with experiment using the information from the total energies and the chemical potentials and draws conclusions on the appropriate reconstruction models for particular atomic environments (As- or Ga-rich).

## II. METHODOLOGY

The surface is modeled by a slab consisting of 16 atomic layers, periodically repeated in the perpendicular direction. Inversion symmetry is imposed on the slab. This eliminates the spurious fields which would otherwise appear in the vacuum region between surfaces of opposite polarity. The atoms are modeled by norm-conserving, nonlocal pseudopotentials, and the total energy for each atomic configuration is calculated by expanding the potentials in a plane-wave basis, using density-functional theory in the local-density approximation for the exchange-correlation energy. Appropriate atomic reservoirs are chosen as sources or sinks of individual atoms for reconstructions with surface stoichiometry different from the ideal. The stoichiometry is defined as  $S = (N_{\text{As}} - N_{\text{Ga}})/4$ , where  $N_{\text{As}}$  ( $N_{\text{Ga}}$ ) is the number of As (Ga) atoms in the first bilayer of the  $(2 \times 2)$  unit cell.

The following guidelines should be kept in mind in the search for structural models: Ga atoms tend to be planar  $sp^2$  bonded when they are threefold coordinated, whereas As atoms tend to be  $p^3$  bonded; semiconducting surfaces characterized by stoichiometry  $S = n/4$ ,  $n$  odd, will in general be preferred over metallic reconstructions. Details of this approach and justification of the guidelines is given in Ref. 13.

III. ( $\bar{1}\bar{1}\bar{1}$ ) SURFACE RECONSTRUCTIONS

Structural models for the reconstructions of this surface are shown in Fig. 1, while the energies and stoichiometries

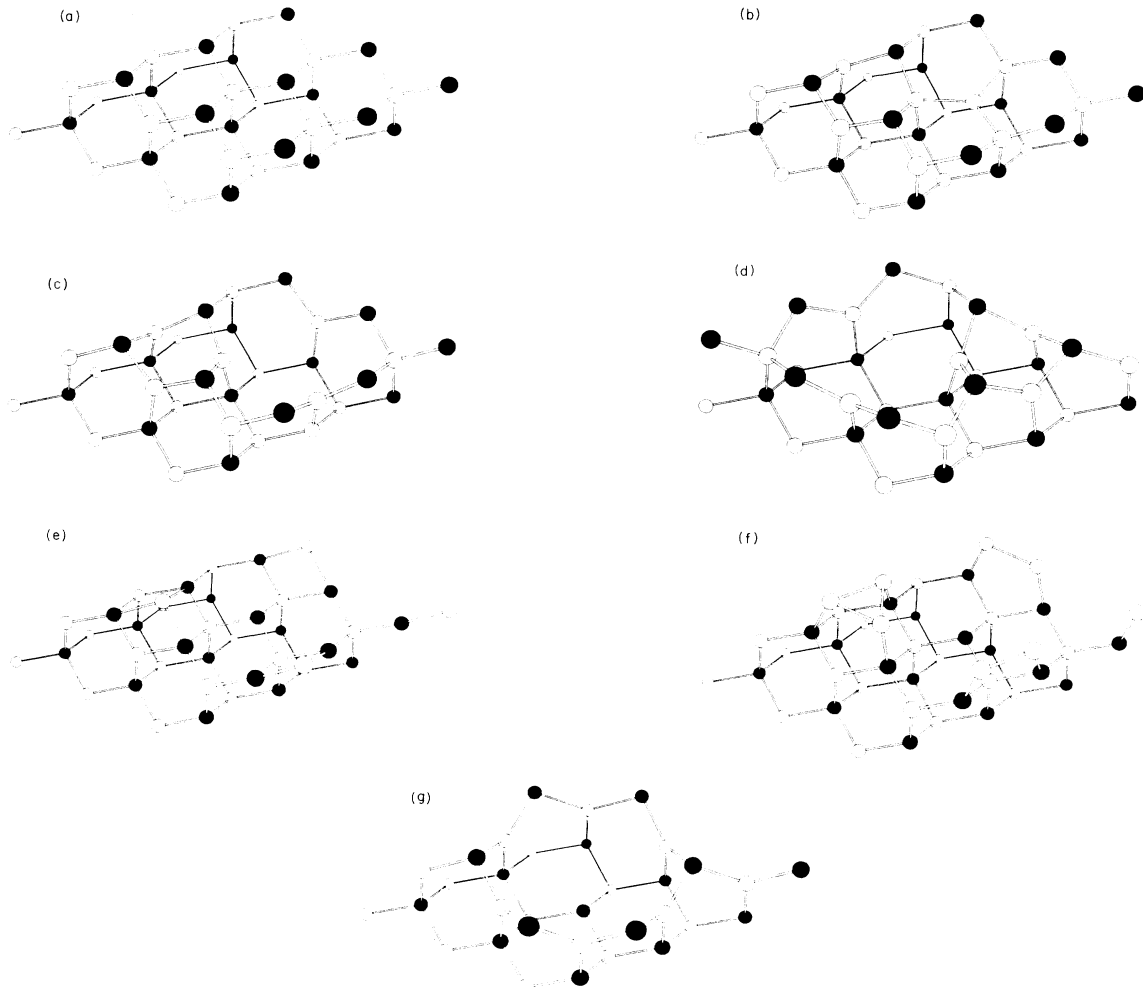


FIG. 1. Structural models for the  $(\bar{1}\bar{1}\bar{1})$  surface  $(2\times 2)$  reconstructions. The first four atomic layers are shown in perspective. The atoms in each layer outline the  $(2\times 2)$  unit cell, in the ideal configuration. The same atoms and their nearest neighbors are shown in the other reconstructions. Solid circles represent As atoms and open circles represent Ga atoms. (a) Ideal surface. (b) Substitutional geometry. (c) Vacancy geometry; a variation of this is the  $\beta$  model. (d) Staggered vacancy geometry; a variation of this is the As tetramer geometry. (e) Adatom geometry; slightly different relaxations apply for the Ga and the As adatoms. (f) Triangle geometry; different relaxations apply for the Ga and the As triangles. (g) Hexagon geometry (6-As, 6-Ga); a variation of this is the puckered hexagon (3-As, 9-Ga).

are given in Table I. In all the cases Ga bulk has been chosen as the Ga atom reservoir (experimental binding energy 2.8 eV per atom<sup>14</sup>), and As<sub>2</sub> gas as the As atom reservoir (experimental binding energy 2.0 eV per atom<sup>14</sup>). The surface is in equilibrium with bulk GaAs (calculated cohesive energy 6.8 eV per pair<sup>13</sup>). The effect of different atomic reservoirs (e.g., As<sub>4</sub>, with experimental binding energy 2.7 eV per atom<sup>14</sup>) will be considered in Sec. IV. Figure 2 shows a schematic band structure of the reconstructions which satisfy the stoichiometric criterion ( $S=n/4$ ,  $n$  odd) for semiconducting character,<sup>13</sup> to establish whether a gap exists (here, as in Ref. 13, the values of the gaps are intended as rough lower bounds).

Figure 1(a) is the ideal unreconstructed  $(\bar{1}\bar{1}\bar{1})$  surface. Buckling<sup>15</sup> on this surface is not energetically favorable: a relaxation similar to the buckling of the (111) surface

[Ref. 13, Fig. 3(b)] would not be appropriate since three out of four surface As atoms would relax to almost planar configurations. The reverse relaxation, with three As atoms moving out of the surface to approach  $p^3$  coordination, leaves the fourth As atom in an unfavorable position, planar with its Ga nearest neighbors. In this case the relaxation energy of the  $p^3$  bonded As atoms is not sufficient to compensate for the unfavorably relaxed As. This latter atom might be substituted by a Ga atom which would actually prefer the planar coordination. The Ga-substitutional model<sup>16</sup> [Fig. 1(b)] is indeed low in energy, despite the fact that three Ga—Ga bonds are formed. It has energy lower than the ideal surface by 2.2 eV, assuming that the removed As atom combines with Ga from the Ga bulk reservoir to form a GaAs pair. This energy is significantly lower than the substitutional model on the

TABLE I. Total energies and stoichiometries for the different  $(2 \times 2)$  reconstruction models of the  $(\bar{1}\bar{1}\bar{1})$  surface. The energies are given in eV per  $(2 \times 2)$  unit cell with respect to the ideal unreconstructed surface. The different models are arranged in stoichiometric classes.

Model geometry	Stoichiometry	Energy
(1) Ga triangle	$-\frac{3}{4}$	-3.5
(2) 3-As, 9-Ga (puckered) hexagon	$-\frac{3}{4}$	-3.0
(3) Ga substitutional	$-\frac{2}{4}$	-2.2
(4) As vacancy + Ga adatom	$-\frac{2}{4}$	-2.2
(5) As vacancy	$-\frac{1}{4}$	-1.9
(6) Staggered As vacancy	$-\frac{1}{4}$	-2.1
(7) $\beta$ model	$-\frac{1}{4}$	0.6
(8) Ga adatom	$-\frac{1}{4}$	-2.2
(9) 6-As, 6-Ga (simple) hexagon	$-\frac{1}{4}$	-1.3
(10) As tetramer	$\frac{1}{4}$	-0.4
(11) As adatom	$\frac{1}{4}$	-0.8
(12) As triangle	$\frac{3}{4}$	-4.5

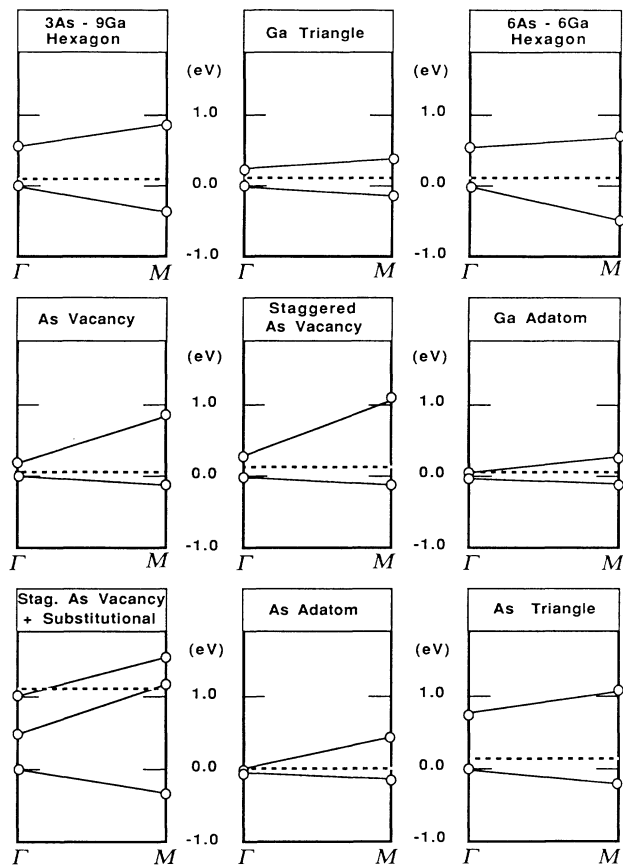


FIG. 2. Schematic band structure for the various reconstruction models which satisfy the stoichiometric criterion for semiconducting character ( $S=n/4$ ,  $n$  odd). The dots are the calculated energies at the  $\Gamma$  and  $M$  points of the surface Brillouin zone. The rest of the bands are linear interpolation of the energy between these two points. The dashed line is the Fermi level.

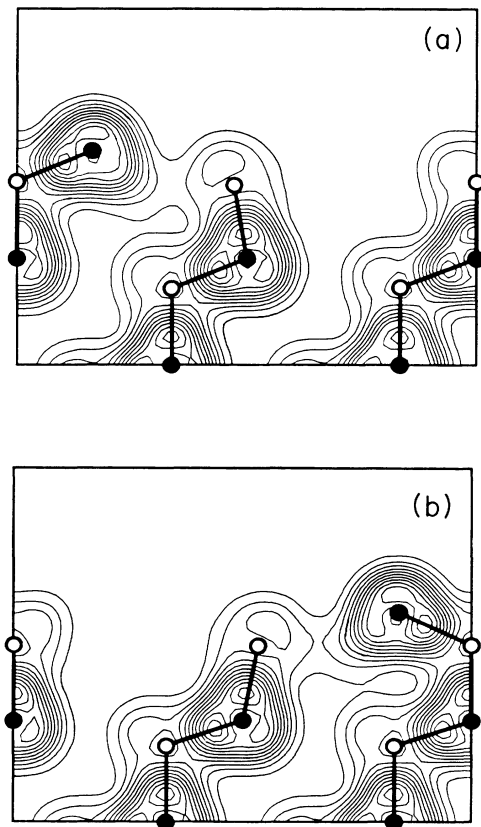


FIG. 3. Charge density of the vacancy models on the  $(110)$  plane which passes through the long diagonal of the  $(2 \times 2)$  unit cell. (a) As-vacancy geometry; (b) Staggered As vacancy.

(111) surface (see Ref. 13), a result in agreement with experimental observations of high sticking coefficient (almost unity) for Ga, compared to that of As which is exceedingly small.<sup>1</sup>

The removal of an As atom, which leads to the vacancy geometry [Fig. 1(c)] does not give an energy gain comparable to the Ga vacancy on the (111) surface.<sup>17</sup> The energy of the As-vacancy geometry is 1.9 eV below the ideal surface [compared to 3.3 eV for the Ga vacancy on the (111) surface, Ref. 13]. The reason for this difference is due mainly to relaxation effects: the relaxation of the Ga atoms around the vacant As site has to be in a direction away from this site, so that they can achieve a planar configuration, while the surface As atoms move outward of the surface toward a  $p^3$  bonding configuration. The three Ga atoms relax over a three-pointed star of bonds on the second layer, distorting the local charge density and thereby reducing the relaxation energy. By contrast, the relaxation of the As atoms outward from the Ga-vacancy site on the (111) surface takes place over an empty hexagon of substrate bonds and the local charge density is not severely distorted. This observation led to the idea of a staggered vacancy: consider the three remaining surface As atoms on the  $(\bar{1}\bar{1}\bar{1})$  surface, rotated by  $60^\circ$  around the common Ga neighbor, in what would be a wurtzitelike succession of planes with a vacancy on the upper plane. Then the Ga atoms would relax to planar configurations away from the vacancy site, over an empty hexagon of substrate bonds, as can be seen in Fig. 1(b). Charge densities on the (110) plane passing through the long diagonal of the  $(2 \times 2)$  surface unit cell, are shown in Fig. 3 for the As-vacancy [Fig. 3(a)] and the staggered As-vacancy [Fig. 3(b)] geometries. A comparison of the two charge distributions indicates how the staggered arrangement might help reduce the energy: the relaxation of the first bilayer Ga atom in the simple As vacancy, reduces the angle between two bonds, which increases the energy due to the repulsive electrostatic interaction. A similar relaxation in the staggered vacancy configuration leads to larger spatial separation between the bond charges, with smaller (if any) energy cost.

The staggered vacancy is indeed lower in energy by 0.2 eV from the simple vacancy, at  $-2.1$  eV with respect to the ideal surface. The question that this result brings to mind is, why does the material not form a wurtzite structure instead of the observed zinc blende? A simple argument is that the staggered configuration has lower energy than the normal one only for the *vacancy relaxation*, and other relaxations do not necessarily exhibit the same behavior. Indeed, the *calculated* energy of the staggered *full* surface plane is higher in energy than the ideal surface by 0.25 eV per  $(2 \times 2)$  unit cell. Both As-vacancy models (normal and staggered) have stoichiometry  $S = -\frac{1}{4}$ , and exhibit semiconducting character (see Fig. 2), with gaps  $\sim 0.15$  and  $\sim 0.32$  eV, respectively.

In the staggered As-vacancy geometry the only atom with severely distorted bonds is the fourfold-coordinated Ga atom in the first bilayer. Substitution of this atom by an As atom leads to a configuration in which an As tetramer in the first bilayer is attached to the surface. This is an interesting possibility since in some experimental MBE

situations the surface is grown by providing a beam of  $\text{As}_4$  molecules. The energy of this model is 0.4 eV lower than the ideal surface, with the missing Ga atom incorporated with excess  $\text{As}_2$  into GaAs bulk. The four As—As bonds of this geometry prohibit a very low-energy reconstruction. The stoichiometry of this model is  $S = \frac{1}{4}$ , but it has metallic character (see Fig. 2), due to the extra electrons from the substitution of a Ga atom by an As atom. If however we assume a  $p$ -type substrate, this reconstruction could exhibit semiconducting character with a gap of  $\sim 0.48$  eV.

The cost of forming like-atom bonds is actually seen better in the  $\beta$  model, a reconstruction proposed by Farrell, Niles, and Bakshi.<sup>18</sup> In this model the surface As atoms are moved to the position of the three Ga atoms adjacent to the As-vacancy site, and vice versa. The rearrangement allows the atoms to relax in a way similar to the (111) surface Ga-vacancy geometry, at the cost of forming three As—As and three Ga—Ga bonds. This model has exactly the same number of atoms as the As vacancy and the staggered As vacancy but is higher in energy than these geometries by 2.4 and 2.6 eV, respectively.

The class of adatom models gives some very interesting reconstructions on the  $(\bar{1}\bar{1}\bar{1})$  surface. The single As adatom is lower than the ideal surface plus excess  $\text{As}_2$  gas by 0.8 eV while the single Ga adatom<sup>19</sup> [Fig. 1(e)] is lower than the ideal surface plus excess Ga bulk by 2.2 eV. However, both models suffer from the same structural problems discussed in connection with the As adatom on the (111) surface. Namely, the direction of the bond between the adatom and the surface deviates significantly from the tetrahedral direction. The local charge density of this bonding arrangement introduces a severe distortion from the usual GaAs bulk bonds. In addition, even though both models satisfy the stoichiometric criterion for being semiconductors ( $S = -\frac{1}{4}$  for the Ga adatom,  $S = \frac{1}{4}$  for the As adatom), they exhibit no gap (see Fig. 2).

The triangle geometries<sup>20</sup> [Fig. 1(f)] are much more stable configurations with nearly perfect atomic coordinations: the adatoms form bonds to the substrate which deviate by a very small amount from the vertical direction and are bonded together in a triangular configuration. The latter bonding should compensate to a large degree for the energy required to remove the atoms from their respective reservoirs (Ga bulk and  $\text{As}_2$  gas for the Ga and As triangles, respectively). As a result the Ga triangle is 3.5 eV lower than the ideal surface, while the As triangle is 4.5 eV lower than the ideal surface. These are actually the two lowest-energy geometries in the two extremes of the stoichiometry  $S$  considered. They are also clearly semiconducting with gaps  $\sim 0.15$  eV for the Ga triangle (stoichiometry  $S = -\frac{3}{4}$ ) and  $\sim 0.76$  eV for the As triangle (stoichiometry  $S = \frac{3}{4}$ ).

Charge-density plots for the adatom models are shown in Figs. 4 and 5. The charge densities of Ga and As adatoms [Fig. 4(a) and 5(a), respectively] show the characteristic distorted bonding arrangement with high local charge density due to single adatoms. The charge densities of Ga and As triangles [Fig. 4(b) and 5(b), respectively] indicate how the triangular arrangement reduces the distortion of the bonds relative to usual GaAs bulk bonds

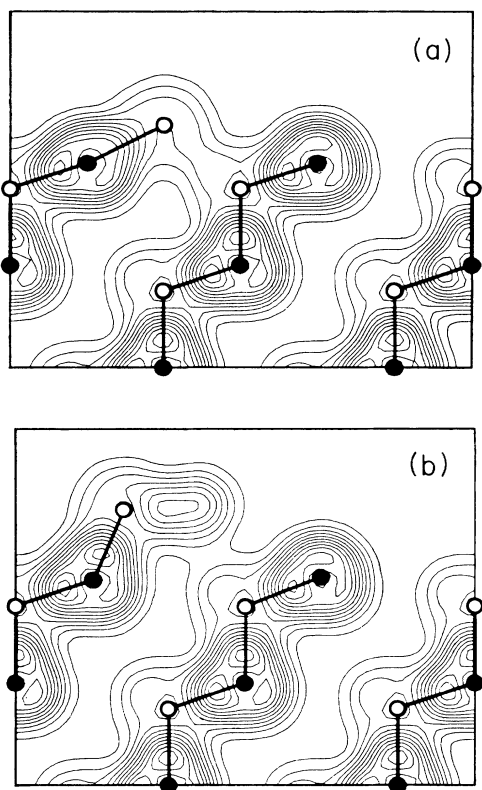


FIG. 4. Charge density of two Ga-adatom geometries in the same plane as Fig. 3. (a) single Ga adatom; (b) Ga triangle.

and thereby leads to more stable, low-energy configurations.

A combination of the As-vacancy and Ga-adatom geometries gives a low-energy configuration (2.2 eV below the ideal surface, provided that the removed As atom combines with excess Ga to form a GaAs pair). In this case, the atomic relaxation of the vacancy is not particularly efficient to begin with, so that addition of the Ga atom does not compete with a strong vacancy induced relaxation [a similar vacancy plus adatom model for the (111) surface is unfavorable due to the competing relaxations<sup>13</sup>]. The number of atoms for this model as well as its energy are identical to the Ga-substitutional geometry discussed above, indicating that the two positions of the Ga atom (substitutional or adatom) are equivalent energetically. Both models have stoichiometry  $S = -\frac{2}{4}$  giving them metallic character.

Finally we turn to a different class of models which permits threefold coordination for all the atoms in the surface bilayer at the expense of removing more atoms from the surface. We call these models hexagon geometries<sup>12</sup> because they are characterized by 12-atom rings in a hexagonal configuration. The atoms are situated at the corners and at the centers of the sides of the hexagon [Fig. 1(g)]. In the 6-As, 6-Ga (or simple) hexagon<sup>21</sup> two As atoms and one Ga atom are missing from the surface bilayer. The remaining Ga atoms are in their usual positions whereas one of the As atoms occupies a normal surface site and the other a staggered surface site. The Ga

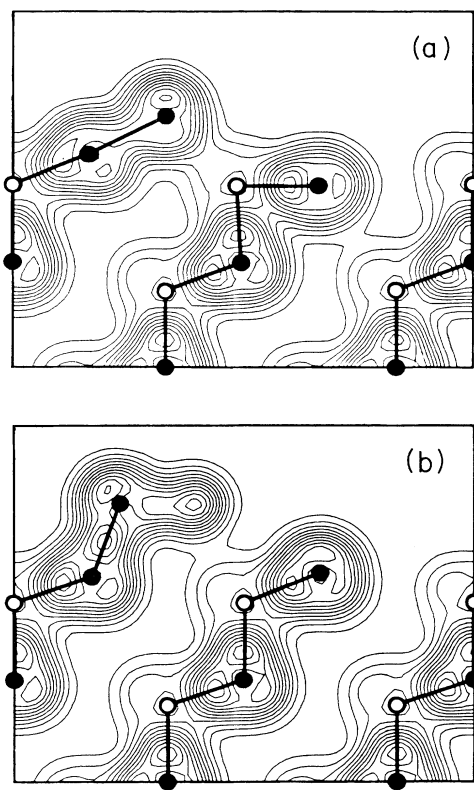


FIG. 5. Charge density of two As-adatom geometries in the same plane as Fig. 3. (a) single As adatom; (b) As triangle.

atoms have all their bonds on the same plane, which is perpendicular to the surface plane. Since they are threefold coordinates, they are ideally bonded with an average angle of  $120^\circ$ . The two surface As atoms are also threefold coordinated but their tendency to form  $p^3$  bonds leads to competing relaxations; that is, an optimized relaxation of one of them destroys the relaxation of the other. Another noticeable feature is that one As atom of the second bilayer is now exposed (situated below the center of the hexagonal ring). Since the atoms around it relax by very small amounts, this particular As atom does not have the chance to achieve an optimal relaxation. This model falls in the same stoichiometric class as the vacancy models (namely  $S = -\frac{1}{4}$ ) since it differs from them by one GaAs pair, which is assumed to be incorporated in the bulk. It exhibits semiconducting character with a gap of  $\sim 0.55$  eV. It is however higher in energy from the vacancy and staggered vacancy geometries by 0.6 and 0.8 eV, respectively.

A possible improvement of the hexagon model is the substitution of one of the surface As atoms by a Ga atom. The site of the substitutional Ga atom should be the normal surface site, since in the staggered one it will interact strongly with the second bilayer atoms directly below it. The relaxation of this Ga atom will then enhance the relaxation of the remaining surface As atom because the two atoms will tend to move in opposite directions. This model falls in the same stoichiometric class with the Ga-triangle model ( $S = -\frac{3}{4}$ ) and consists of a 3-As, 9-Ga (or

puckered) hexagon. Its character is semiconducting with a gap of  $\sim 0.53$  eV. Its energy is 0.5 eV higher than the Ga triangle, at  $-3.0$  eV with respect to the ideal surface plus excess Ga bulk, after forming GaAs pairs with the three removed As atoms and the available Ga.

Charge densities for the two hexagon geometries are shown in Fig. 6. The plane of the figures is the same as in previous charge-density plots, with the second bilayer exposed As atom at the right and left edges. The simple hexagon [Fig. 6(a)] consists of planar Ga atoms bonded to two surface As atoms which inhibit perfect relaxation of each other. In the puckered hexagon [Fig. 6(b)] one of the surface As atoms has been replaced by a Ga atom which enhances the relaxation of the other As atom at the cost of three Ga—Ga bonds.

Since the comparison of the energy of the simple hexagon to that of the As vacancy involves the calculated cohesive energy of a bulk GaAs pair, it is important to ask how does the size of the plane wave basis affect the energy differences quoted above. It is well known that an increase in the basis set will give a lower cohesive energy (from the variational principle). A lower cohesive energy will in turn favor the hexagon geometry over the vacancy, because one GaAs pair is removed from the latter and incorporated into the bulk. We have therefore performed a study of the energy differences as a function of the basis set size. The size is determined by the energy cutoffs for the plane waves,  $E_1$  and  $E_2$  (defined in Ref. 13, Sec. II).

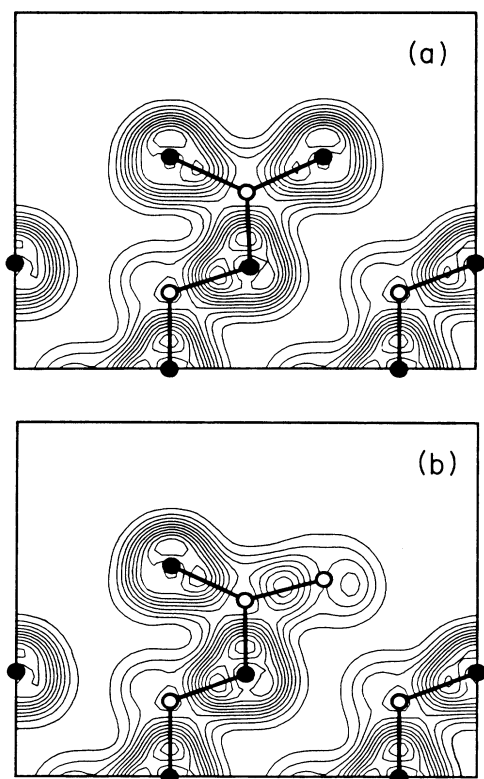


FIG. 6. Charge density of two hexagon geometries in the same plane as Fig. 3. (a) simple hexagon (6-As, 6-Ga atoms); (b) puckered hexagon (3-As, 9-Ga atoms).

Thus the calculations were done at  $(E_1, E_2) = (2, 4), (3, 6), (4, 8),$  and  $(5, 10)$  Ry, and the results are shown in Fig. 7. Except for the unreliably small energy cutoff of  $(E_1, E_2) = (2, 4)$  Ry, the results of the calculations indicate that energy differences are remarkably well converged. Thus, even though the cohesive energy of GaAs bulk changes by 1.0 eV per pair (as expected) when going from  $(E_1, E_2) = (4, 8)$  to  $(5, 10)$  Ry, the energy differences are identical to within 0.05 eV between the vacancy and staggered vacancy, and to within 0.1 eV between the staggered vacancy and the hexagon. It is also important to notice that the cohesive energy of GaAs at  $(E_1, E_2) = (4, 8)$  Ry (where the rest of the calculations were performed) is, fortuitously, very close to the experimental value. This indicates that use of the experimental values for the Ga bulk and  $\text{As}_2$  gas binding energies is justified in the context of the present work. The conclusion to be drawn from this energy convergence study is that the calculated cohesive energy of a pair of Ga and As atoms is roughly the same, whether they form part of the surface or of the bulk; put differently, the inherent errors of the pseudopotential local-density-functional formalism are the same for the surface and bulk calculations, and therefore it is reasonable to consider bulk GaAs as a reservoir for the displaced surface atoms. Finally, the energy convergence study gives a measure of the errors (due to the limited basis set) involved in comparing surfaces with *different* numbers of atoms: they are of the order of 0.1 eV. Error bars due to the uncontrolled approximations of the method are estimated to be also 0.1 eV, giving a total error bar of the

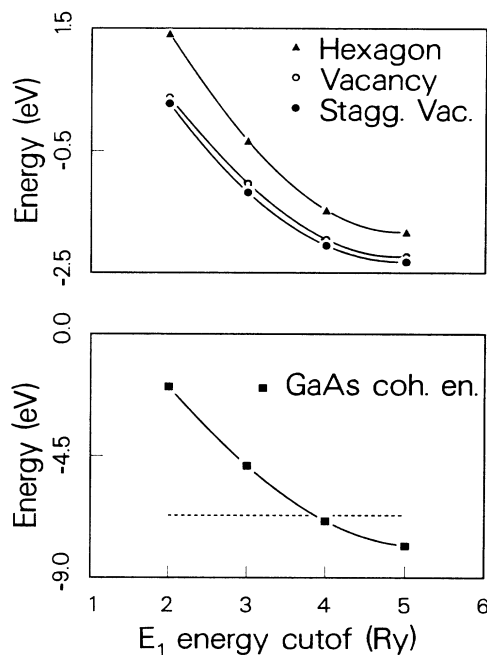


FIG. 7. Energy differences as a function of plane-wave basis cutoff. Upper panel: energy of three reconstruction models of the  $(\bar{1}\bar{1}\bar{1})$  surface, in eV per  $(2 \times 2)$  unit cell. Lower panel: cohesive energy of bulk GaAs in eV per pair. The dashed line represents the experimental value (6.7 eV). Notice the different vertical energy scales for the two panels.

order of 0.2 eV for surfaces with different number of atoms. In the case of surfaces with the *same* number of atoms the error bar is only the latter 0.1 eV.

#### IV. EFFECT OF RELATIVE CHEMICAL POTENTIAL

The total energy of each configuration up to this point has been given assuming the atomic reservoirs to be Ga bulk for Ga-rich surface reconstructions and As<sub>2</sub> gas for As-rich surface reconstructions. In either case equilibrium with GaAs bulk is assumed. This situation however does not cover the whole range of experimentally accessible environments. In particular As-rich surface reconstructions can be stable under Ga-rich environment and vice versa. In order to account for this we let the relative chemical potential  $\delta\mu$  vary between its value in the Ga-rich environment and that in the As-rich environment. The range of values for  $\delta\mu$  is  $[-1.0 \text{ eV}, 1.0 \text{ eV}]$ , as explained in Ref. 13. The total energy of the various surface reconstructions is then given in terms of  $\delta\mu$  and the stoichiometry  $S$ , by

$$E_{\text{As-rich}}(\delta\mu) = E_{\text{As-rich}}^{\text{eq.}} + 4S(1.0 \text{ eV} - \delta\mu),$$

$$E_{\text{Ga-rich}}(\delta\mu) = E_{\text{Ga-rich}}^{\text{eq.}} - 4S(1.0 \text{ eV} + \delta\mu),$$

where  $E_{\text{As-rich}}^{\text{eq.}}$  and  $E_{\text{Ga-rich}}^{\text{eq.}}$  are the total energies of the As-rich ( $S > 0$ ) and Ga-rich ( $S < 0$ ) surfaces in equilibrium with As<sub>2</sub> and Ga bulk environments as given in Table I.

These considerations give a more complete picture of the reconstruction energies for the  $(\bar{1}\bar{1}\bar{1})$  surface under all possible environments, which is depicted graphically in Fig. 8. The dashed line indicates the upper limit of the  $\delta\mu$  range if we had considered As<sub>4</sub> to be the As reservoir. The intersection of this dashed line with the total-energy curves gives the energy of each reconstruction for the As<sub>4</sub> reservoir. We can conclude that this choice of atomic reservoirs does not alter qualitatively the relative energies since the lowest-energy reconstruction for either As reser-

voir (As<sub>2</sub> or As<sub>4</sub>) in the As-rich region ( $\delta\mu > 0.0 \text{ eV}$ ) is the As triangle. Furthermore if the reservoir restrictions are removed and  $\delta\mu$  scans the entire possible range assuming only equilibrium with bulk GaAs (in which case  $\delta\mu \in [-3.8, 3.0 \text{ eV}]$ , see Ref. 13), no new crossings between the lowest-energy curves are encountered.

From Fig. 8 *alone* we can predict that phase transitions will occur as the relative chemical potential  $\delta\mu$  scans its range, whenever two lowest-energy lines cross and different reconstructions become the lowest-energy configuration. Two such crossings occur in Fig. 8. At this point, however, it is important to recall that our search was restricted to a subset of  $(2 \times 2)$  reconstructions (the large number of models examined does not necessarily exhaust all the possibilities). There might actually exist more complicated patterns in which atoms are rearranged once a particular configuration has become energetically unstable. It is necessary therefore to examine the available experimental information about such structural transitions, in conjunction with the total energy versus chemical potential curves before attempting to propose particular models for the reconstructions.

#### V. STRUCTURAL PHASE TRANSITIONS

The transitions occurring on this surface as the relative supply of As and Ga atoms is changed, are easy to observe experimentally and much more dramatic than what is observed on the (111) surface: the As-rich environment reconstruction is  $(2 \times 2)$ , but reverts to a  $(\sqrt{19} \times \sqrt{19})$  geometry when  $\sim 0.44$  of an As monolayer is desorbed by heating.<sup>1,2</sup> Another  $(2 \times 2)$  reconstruction with still lower As content has been reported recently, obtained through simultaneous ion bombardment and annealing at high temperatures.<sup>9</sup>

We can interpret these experimental observations using the energy versus chemical potential curves of Fig. 8. These curves however cannot be used as the sole input because they do not include kinetic effects which could be crucial in certain cases. Thus the low sticking coefficient of As indicates it is unlikely that As-adatom models (either the single As adatom or the As triangle) are stable on the As-terminated surface. It may in fact be rather difficult to simulate the surface As-rich environment. The experimentally observed As-rich reconstruction should be one of the two lowest-energy geometries in the  $\delta\mu \in [-0.3, -0.1] \text{ eV}$  range, i.e., either the staggered As vacancy or the Ga adatom (assuming higher values of  $\delta\mu$  to be beyond the experimentally explored conditions). We are inclined to favor the staggered As vacancy over the Ga adatom which is structurally unfavorable as argued above (the fact that the staggered vacancy lies 0.1 eV higher than the Ga adatom is not significant in view of the calculational uncertainty which, as argued in Sec. VI, is of the order of 0.2 eV). On the other hand, the Ga-rich reconstruction is most likely the Ga triangle, both from energetic and structural considerations. It is the lowest-energy geometry among all the negative stoichiometry models and presents the most favorable atomic coordination once all the surface As and part of the surface Ga has been removed.

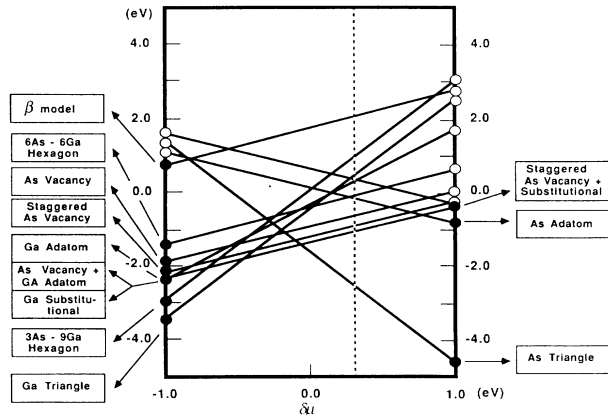


FIG. 8. Energy versus relative chemical potential  $\delta\mu$  of the different reconstruction models of the  $(\bar{1}\bar{1}\bar{1})$  surface. The range of  $\delta\mu$  scans the values consistent with the Ga bulk and As<sub>2</sub> gas reservoirs. The closed dots are the calculated energies per  $(2 \times 2)$  unit cell with respect to the ideal surface. The dashed line indicates the upper limit of  $\delta\mu$  consistent with an As<sub>4</sub> gas reservoir.

Our calculations indicate that a transition should occur between the Ga triangle and the staggered As vacancy at  $\delta\mu \sim -0.3$  eV upon desorption of 0.50 of an As monolayer from the latter. The stable  $(\sqrt{19} \times \sqrt{19})$  geometry on the other hand is obtained from the As-rich reconstruction upon desorption of  $\sim 0.44$  of an As monolayer.<sup>2</sup> We can infer that the  $(\sqrt{19} \times \sqrt{19})$  geometry is a low-energy metastable reconstruction, lying in stoichiometry between the Ga triangle and the staggered As vacancy. Total-energy calculations on the  $(\sqrt{19} \times \sqrt{19})$  geometry are not feasible at present. Nevertheless, based on the above considerations we propose a  $(\sqrt{19} \times \sqrt{19})$  geometry which embodies features of both the Ga-triangle and the staggered As-vacancy configurations (models for this reconstruction have also been proposed by Ranke and Jacobi, Ref. 10).

The  $(\sqrt{19} \times \sqrt{19})$  geometry is constructed in the following way: Starting with the staggered vacancy we can remove the three As atoms shown in the  $(2 \times 2)$  unit cell of Fig. 9(a). A large triangular unit can then be identified and is shown by dashed lines in Fig. 9(a). This unit contains ten Ga atoms and six As atoms. Rearrangement of the As atoms and displacement of the central Ga atom allows the formation of three smaller, energetically favorable Ga triangle units. This in turn suggests that the large triangle itself, may be a low-energy building block for a larger surface reconstruction. Indeed, a close packing arrangement of such triangles leads immediately to a  $(\sqrt{19} \times \sqrt{19})$  structure as indicated in Fig. 9(b).

The final proposed reconstruction, shown in Fig. 9(b), consists of six As atoms and nineteen Ga atoms in the first bilayer of the  $(\sqrt{19} \times \sqrt{19})$  unit cell. All the surface As atoms are threefold coordinated, including the one exposed As atom in the second bilayer [situated at the center of the large triangle, Fig. 9(b)]. The surface Ga atoms are threefold or fourfold coordinated. The composition of the surface layer is in agreement with available experimental information. In particular, no Ga atoms desorb during the transition from the As-stabilized  $(2 \times 2)$  reconstruction

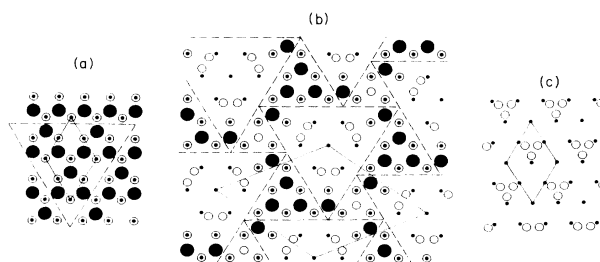


FIG. 9. Structural transitions on the  $(\bar{1}\bar{1}\bar{1})$  surface: (a) the As-rich environment  $(2 \times 2)$  reconstruction, staggered As vacancy. (b) the metastable  $(\sqrt{19} \times \sqrt{19})$  reconstruction. (c) the Ga-rich environment  $(2 \times 2)$  reconstruction, Ga triangle. Closed circles represent As atoms, empty circles represent Ga atoms. A closed circle inside an open one represents an As atom directly below a Ga atom. The size of the circles indicates proximity of the atoms to the surface. The relaxation is schematic for (c) and omitted for the other models.

to the  $(\sqrt{19} \times \sqrt{19})$  geometry.<sup>2</sup> Furthermore, the amount of As desorbing during this transition is 0.43 of a monolayer, in excellent agreement with experiment.<sup>2</sup> Finally, we note that any  $(\sqrt{19} \times \sqrt{19})$  geometry must be metallic because of symmetry constraints. The structure we propose is very weakly metallic with an excess of only  $\frac{3}{4}$  of an electron per  $(\sqrt{19} \times \sqrt{19})$  unit cell. If all the As is removed from the surface by heating and ion bombardment, the Ga triangle should be obtained as shown in Fig. 9(c).

#### ACKNOWLEDGMENTS

This work was supported in part by U.S. Joint Service Electronics Program (JSEP) Contract No. DAAL-03-86-K-0002. One of us (E.K.) should like to thank the IBM Thomas J. Watson Research Center (Yorktown Heights, NY) for its hospitality while portions of this work were carried out, and acknowledge partial support by IBM.

<sup>1</sup>A. Y. Cho and I. Hayashi, *Solid-State Electron* **14**, 125 (1971).

<sup>2</sup>J. R. Arthur, *Surf. Sci.* **43**, 449 (1974).

<sup>3</sup>K. Jacobi, G. Steinert, and W. Ranke, *Surf. Sci.* **57**, 571 (1976).

<sup>4</sup>K. Jacobi, C. v. Muschwitz, and W. Ranke, *Surf. Sci.* **82**, 270 (1979).

<sup>5</sup>S. Y. Tong, G. Xu, and W. N. Mei, *Phys. Rev. Lett.* **52**, 1693 (1984).

<sup>6</sup>R. D. Bringans and R. Z. Bachrach, *Phys. Rev. Lett.* **53**, 1954 (1984).

<sup>7</sup>J. Bohr, R. Feidenhans'l, M. Nielsen, M. Toney, R. L. Johnson, and I. K. Robinson, *Phys. Rev. Lett.* **54**, 1275 (1985).

<sup>8</sup>A. D. Katnani and D. J. Chadi, *Phys. Rev. B* **31**, 2554 (1985).

<sup>9</sup>M. Alonso, F. Soria, and J. L. Sacedon, *J. Vac. Sci. Technol. A* **3**, 1595 (1985).

<sup>10</sup>W. Ranke and K. Jacobi, *Surf. Sci.* **63**, 33 (1977).

<sup>11</sup>J. D. Chadi, *Phys. Rev. Lett.* **57**, 102 (1986).

<sup>12</sup>E. Kaxiras, Y. Bar-Yam, J. D. Joannopoulos, and K. C. Pan-

dey, *Phys. Rev. Lett.* **57**, 106 (1986).

<sup>13</sup>E. Kaxiras, Y. Bar-Yam, J. D. Joannopoulos and K. C. Pandey, preceding paper, *Phys. Rev. B* **35**, 9625 (1987).

<sup>14</sup>R. Hultgren *et al.*, *Selected Values of the Thermodynamic Properties of the Elements* (American Society of Metals, Metals, Park, Ohio, 1973).

<sup>15</sup>D. Haneman, *Phys. Rev.* **121**, 1093 (1961).

<sup>16</sup>A. U. MacRae and G. W. Gobeli, *J. Appl. Phys.* **35**, 1629 (1964).

<sup>17</sup>Proposed by S. Y. Tong, G. Xu, and W. N. Mei, see Ref. 5, and by D. J. Chadi, *Phys. Rev. Lett.* **52**, 1911 (1984).

<sup>18</sup>H. Farrell, D. W. Niles, and M. H. Bakshi (unpublished).

<sup>19</sup>W. A. Harrison, *J. Vac. Sci. Technol.* **16**, 1492 (1979).

<sup>20</sup>E. Kaxiras, K. C. Pandey, Y. Bar-Yam, and J. D. Joannopoulos, *Phys. Rev. Lett.* **56**, 2819 (1986).

<sup>21</sup>This model is identical to the multivacancy model proposed by J. D. Chadi, see Ref. 11.